Electron-electron interactions in the conductivity of graphene

A. A. Kozikov,[1] A. K. Savchenko,[1] B. N. Narozhny,[2] and A. V. Shytov[1]
[1]*School of Physics, University of Exeter, Exeter, EX4 4QL, United Kingdom*
[2]*Institut für Theorie der Kondensierten Materie, Karlsruher Institut für Technologie, 76128 Karlsruhe, Germany*
(Received 27 July 2010; published 24 August 2010)

The effect of electron-electron interaction on the low-temperature conductivity of graphene is investigated experimentally. Unlike in other two-dimensional systems, the electron-electron interaction correction in graphene is sensitive to the details of disorder. A temperature regime of the interaction correction is identified where quantum interference is partially suppressed by intravalley scattering. We determine the value of the interaction parameter, $F_0^\sigma \simeq -0.1$, and show that its small value is due to the chiral nature of interacting electrons.

DOI: 10.1103/PhysRevB.82.075424 PACS number(s): 73.23.−b, 72.15.Rn, 73.43.Qt

I. INTRODUCTION

The low-temperature behavior of the resistance of electron systems is determined by quantum effects. Two distinct phenomena are responsible for this: quantum interference of electron waves scattered by impurities[1] (weak localization, WL), and electron-electron interaction (EEI) in the presence of disorder.[2] The WL correction is used to study electron dephasing, while the EEI correction, which is not sensitive to dephasing, has been used to probe the dynamics of interacting electrons, e.g., Refs. 3–8. In graphene, the charge carriers are chiral and located in two valleys. As a result, WL is sensitive not only to inelastic (phase breaking) scattering but also to a number of elastic scattering mechanisms.[9,10] For this reason, the WL correction to the conductivity can be either negative or positive, depending on the experimental conditions.[11,12] So far the effects of EEI on the low-temperature conductivity of graphene have not been studied experimentally and only the high-temperature ballistic regime was analyzed theoretically.[13]

In the ballistic regime, $k_B T\tau_p > 1$, where τ_p is the momentum relaxation time, the EEI correction is determined by coherent backscattering on a single impurity, which is suppressed due to the chirality of charge carriers.[14] As a result, the EEI correction can only occur due to scattering on atomically sharp defects and is expected to have a universal form which is independent of the details of the interaction. In addition, the ballistic regime in graphene can only be realized at relatively high temperatures, where the EEI effect has to be separated from strong effects of electron-phonon scattering. Thus this regime is not expected to be promising for the study of electron interactions in graphene.

In the diffusive regime, $k_B T\tau_p < 1$, interacting electrons in graphene scatter on multiple impurities so that backscattering is less important. Hence the EEI correction will contain information about the details of interaction. In this work we study the EEI effect on the conductivity of graphene in this regime. We show that our results are described by a logarithmic correction to the conductivity[2]

$$\delta\sigma^{\mathrm{EEI}}(T) = -A(F_0^\sigma)\frac{e^2}{2\pi^2\hbar}\ln\frac{\hbar}{k_B T\tau_p}. \tag{1}$$

Here the coefficient $A(F_0^\sigma)$ is determined by the strength of interaction and the symmetry of electron states. We show that in graphene there is a new regime of EEI and find the value of the interaction parameter F_0^σ.

II. EXPERIMENTAL METHODS

Three samples with Hall-bar geometry (S1, S2, and S3) were fabricated by mechanical exfoliation[15] of graphite on Si substrates covered by 300 nm of SiO_2. Sample parameters are shown in Table I. Quantum-Hall-effect measurements were performed to verify that the samples are monolayers.[15] Figure 1 shows the resistivity ρ as a function of the gate voltage for the three samples. The bars indicate three regions of the gate voltage where $\rho(T)$ was measured in all samples: $V_g = 3$, 16, and 36 V with respect to the Dirac point (maximum in the resistance).

Figure 2(a) shows $\rho(T)$ in sample S1 in the temperature range $T = 5-200$ K. The temperature dependence of the resistivity $\rho(T)$ is due to both quantum corrections and classical electron-phonon scattering.[16,17] In order to study the quantum corrections, we first subtract the phonon contribution to $\rho(T)$, as described below. The Boltzmann transport theory[18] gives the following expression for the electron-acoustic phonon interaction contribution:

$$\rho_{ph}(T) = \frac{1}{\pi}\frac{D_a^2 E_F^2}{\rho_s v_{ph}\hbar^3 v_F^3}\int_0^\pi \frac{T_{\mathrm{BG}}}{T}\cos^2\frac{\theta}{2}\sin^4\frac{\theta}{2} \times \sinh^{-2}\left(\frac{T_{\mathrm{BG}}}{T}\sin\frac{\theta}{2}\right)d\theta, \tag{2}$$

where D_a is the deformation potential, T_{BG}

TABLE I. Electron mobility μ (in $\mathrm{cm^2\ V^{-1}\ s^{-1}}$) at 5 K for three regions of the carrier density in samples S1, S2, and S3. Characteristic scattering times τ_i and τ_* (in ps) are also shown for sample S1.

	S1			S2	S3
Region	μ	τ_i	τ_*	μ	μ
I	17500	14	0.45	9300	12500
II	11500	3	0.3	5400	11000
III	9700	1	0.35	4500	9500

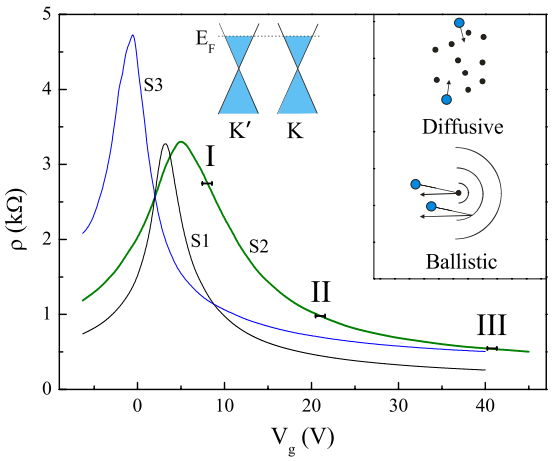

FIG. 1. (Color online) The gate voltage dependence of the resistivity for samples S1, S2, and S3. The bars (shown for S2) indicate three studied regions. Insets: graphene band structure with two valleys and a schematic illustration of the regimes of interaction between two electrons that are scattered by impurities.

$=2v_{ph}E_F/(\hbar k_B v_F)$ is the Bloch-Grüneisen temperature, θ is the scattering angle, $\rho_s=7.6\times10^{-7}$ kg m^{-2} is the density of graphene, $v_{ph}=2\times10^4$ m s^{-1} is the speed of sound, $v_F=10^6$ m s^{-1} is the Fermi velocity of carriers, and E_F is the Fermi energy. In the high-temperature limit, $T\gg T_{\mathrm{BG}}$, the phonon contribution to the resistivity is

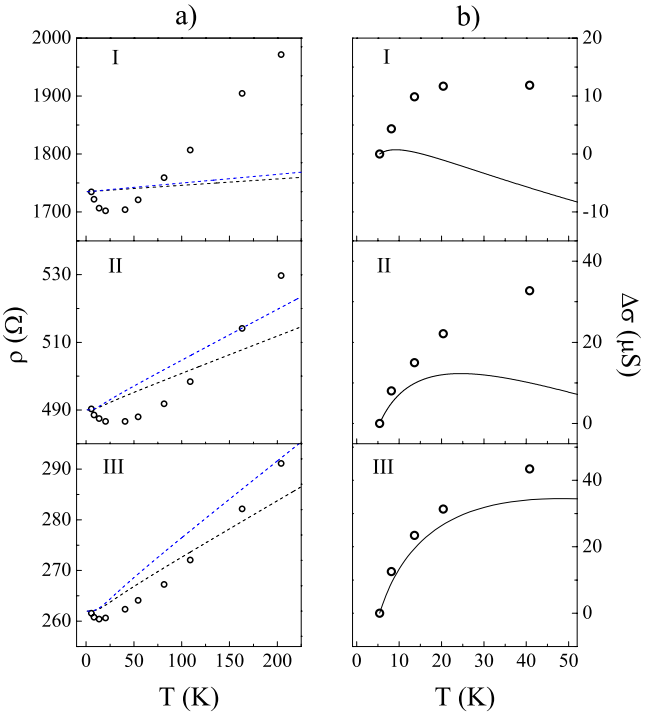

FIG. 2. (Color online) (a) The resistivity as a function of temperature for sample S1 for three regions of carrier density. The dashed lines indicate the magnitude of the acoustic phonon contribution calculated using Eq. (2) (shifted for convenience) with $D_a=18$ (black) and 21 eV (blue). (b) The conductivity after the phonon contribution with $D_a=18$ eV has been subtracted. Solid lines show the WL correction found from Eq. (4).

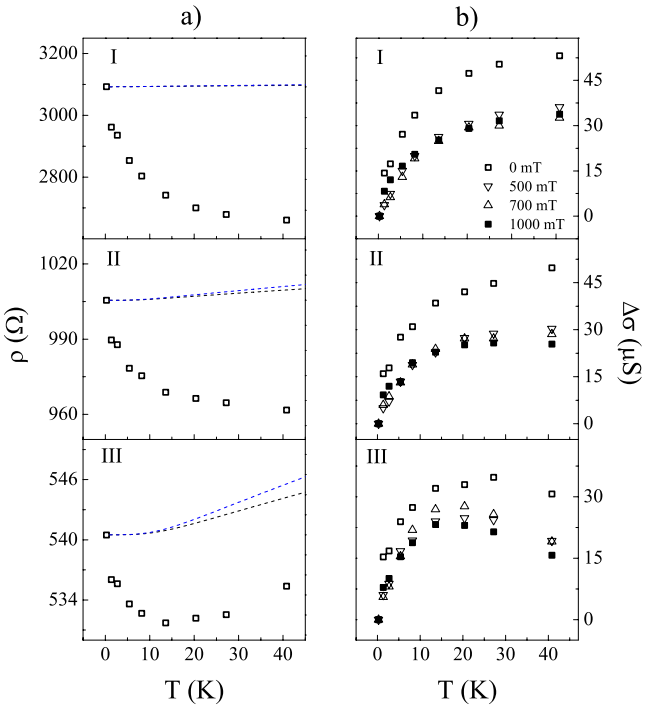

FIG. 3. (Color online) (a) The resistivity as a function of temperature for sample S2, shown for three regions. The dashed lines indicate the magnitude of the acoustic phonon contribution calculated using Eq. (2) (shifted for convenience) with $D_a=18$ (black) and 21 eV (blue). (b) The conductivity $\Delta\sigma(T)=\sigma(T)-\sigma(T_0)$ at different magnetic fields (the contribution of acoustic phonons with $D_a=18$ eV has been subtracted).

$$\rho_{ph}(T)=\left(\frac{h}{e^2}\right)\frac{\pi^2 D_a^2 k_B T}{2h^2\rho_s v_{ph}^2 v_F^2}. \tag{3}$$

In Ref. 17 high-T resistivity data were fitted with $D_a=18\pm1$ eV. In Ref. 19 two different values of the deformation potential were used for electrons and holes: $D_a=18$ and 21 eV, respectively. In our experiment we find[20] the value of the deformation potential to be 18 eV. Following Ref. 4 we have subtracted the phonon contribution given by Eq. (2). Here D_a is the only adjustable parameter and $T_{\mathrm{BG}}=25$, 60 and 90 K for regions I, II, and III, respectively. We repeat this procedure also for $D_a=21$ eV to check its robustness. Figures 2(a) and 3(a) show that the relative magnitude of the phonon contribution depends both on the carrier density and sample quality (mobility). In region I, in all studied samples, it accounts for less than 5% of the change in $\rho(T)$ for temperatures below 50 K and the subtraction procedure is not necessary. In region III, where the carrier density is high and the resistivity is low, the phonon contribution is important and the value of the electron-electron interaction correction becomes sensitive to the choice of D_a. In region II it is significant in the high-mobility sample S1 and less important in the low-mobility sample S2.

The resulting quantum correction to the conductivity is shown for all regions in Figs. 2(b) and 3(b) as $\Delta\sigma(T)=\sigma(T)-\sigma(T_0)$, where T_0 is the lowest studied temperature, $\sigma(T)=[\rho(T)-\rho_{ph}(T)]^{-1}$. The analysis has been limited to the range $T<50$ K in order to rule out other types of phonons at higher temperatures.[16,17]

To separate the correction due to EEI from that due to WL, we combine measurements of the temperature dependence of the conductivity with studies of magnetoresistance. The separation has been performed by two methods. In the first method, used to analyze the results of samples S1 and S3, the low-field perpendicular magnetoresistance has been measured, in order to determine the characteristic times responsible for WL: the inelastic dephasing time $\tau_\varphi(T)$, the elastic time of intervalley scattering τ_i, and the elastic time τ_* which describes intravalley suppression of quantum interference (due to topological defects and "trigonal" warping of the energy spectrum[10]). (This analysis is done following the method described in Refs. 11 and 12.) These times are used to determine the WL correction[10] $\delta\sigma^{\mathrm{WL}}(T)$

$$\delta\sigma^{\mathrm{WL}}(T) = -\frac{e^2}{2\pi^2\hbar}\left\{\ln[1+2\tau_\varphi(T)/\tau_i] - 2\ln\left[\frac{\tau_\varphi(T)/\tau_p}{1+\tau_\varphi(T)/\tau_i+\tau_\varphi(T)/\tau_*}\right]\right\}, \quad (4)$$

which is then subtracted. In the second method, used to analyze sample S2, the EEI correction has been isolated by suppressing WL by a perpendicular magnetic field. The magnetic field, which is enough to suppress interference, is still too small to affect the EEI correction.[1] Both methods lead to close results for the magnitude of the EEI correction in the studied samples, which proves the robustness of the first method based on Eq. (4).

The solid line in Fig. 2(b) shows the WL correction to the conductivity, $\Delta\delta\sigma^{\mathrm{WL}}(T)=\delta\sigma^{\mathrm{WL}}(T)-\delta\sigma^{\mathrm{WL}}(T_0)$, found from the analysis of the magnetoresistance using the first method. One can see that the two types of quantum correction, WL and EEI, are of similar magnitude. The solid lines show clearly that in regions I and II there is a transition from weak localization, an increase of $\Delta\sigma(T)$, to antilocalization, a decrease in $\Delta\sigma(T)$. (Earlier, such a transition was detected in the change of the sign of magnetoresistance[12] with the transition temperatures of ~10 K in region I and ~25 K in region II, which is in agreement with this experiment.)

Figure 3(a) shows the temperature dependence of the resistivity of sample S2 in the temperature range 0.25–40 K. First, the phonon contribution, Eq. (2), shown by the dashed line is subtracted in regions II and III. The remaining quantum contribution to the conductivity is presented in Fig. 3(b), for different magnetic fields. One can see that with increasing B there is a decrease in the slope of the temperature dependence until a saturation is reached. This is a signature that the WL correction has been suppressed.

The suppression of WL is expected at fields which are much larger than the so-called transport field $B_{tr}=\hbar/2el_p^2$, where l_p is the mean-free path.[21] For sample S2 the values of B_{tr} are 120, 70 and 45 mT for regions I, II, and III, respectively, and therefore it is not surprising that WL appears to be suppressed at $B=1$ T, Fig. 3(b). On the other hand, the effect of the magnetic field on the EEI correction is due to the Zeeman splitting of the triplet "channel" and is expected at higher fields,[2] $g^*\mu_B B > k_B T$, where g^* is the Landé g-factor, and μ_B is the Bohr magneton. For the g-factor in graphene[22]

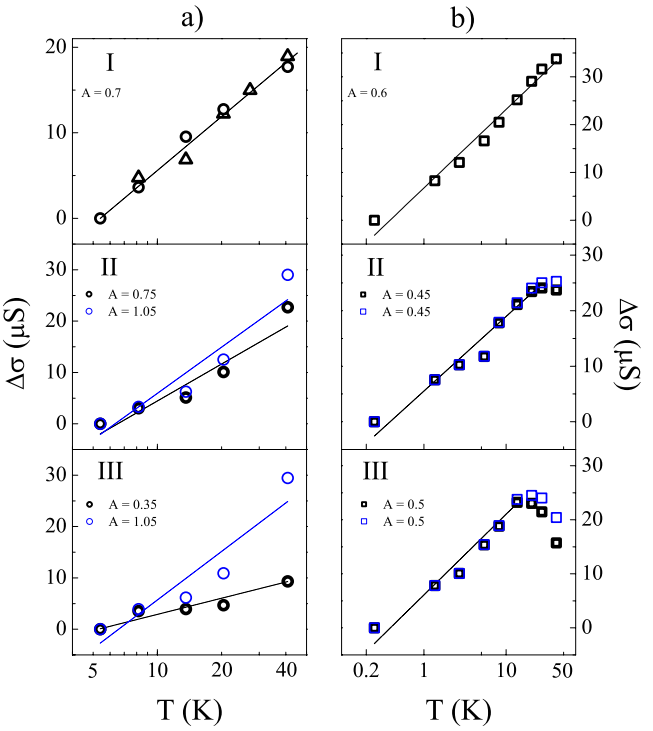

FIG. 4. (Color online) The electron-electron interaction correction to the conductivity. (a) The results for sample S1 (circles) are obtained by determining the WL correction using Eq. (4) (in region I the results for sample S3 are also displayed by triangles). (b) For sample S2 the WL contribution is suppressed by magnetic field. Solid lines are fits to Eq. (1). Black and blue colors correspond to the subtraction of Eq. (2) with D_a=18 eV and 21 eV, respectively.

~2 and temperatures above 1 K, this condition is satisfied at fields higher than 1 T.

The extracted EEI correction is shown for samples S1 and S2 in Fig. 4, where we also add the result for sample S3 in region I. We have shown the uncertainty arising from different values of D_a to illustrate the stability of our results in the high-mobility sample S1 at low carrier densities (regions I and II) and in the low-mobility sample S2 at all studied densities. The EEI correction is indeed logarithmic in temperature, Eq. (1), with close values of A, A=0.45–0.75 with an error of 10%, for the majority of regions of the carrier density in the studied samples.

III. DISCUSSION

To interpret the obtained value of A, we note that the theory[2] distinguishes between the contributions from different quantum states of two interacting electrons, commonly referred to as channels. The coefficient A takes the form $A=1+c[1-\ln(1+F_0^\sigma)/F_0^\sigma]$, where F_0^σ is the Fermi-liquid constant. While the first term in this relation represents the universal contribution of the "singlet" channel, the second (Hartree) term describes the contributions of c "triplet" channels. For example, in a single-valley two-dimensional (2D) system (such as in GaAs) the coefficient $c=3$ due to identical contributions of three spin triplet states. (When the this degen-

eracy is lifted by magnetic field,[2] two components become suppressed, resulting in $c=1$.)

In two-valley 2D systems [e.g., in Si-metal-oxide-semiconductor field-effect transistors (MOSFETs) (Refs. 7 and 8)] the situation is more complicated. In the absence of intervalley scattering, the valley index $v=\pm$ is a good quantum number. In this case the overall number of channels is 16, due to fourfold spin degeneracy of two interacting electrons and an additional fourfold degeneracy due to the two valleys. This gives the prefactor $c=15$. This result also holds if the intervalley scattering is weak, $k_BT \gg \hbar/\tau_i$, i.e., when the typical electron energy is larger than the characteristic rate of intervalley scattering. However, at low temperatures, $k_BT \ll \hbar/\tau_i$, strong intervalley scattering mixes the valleys and A takes the same form as in the single-valley case.

Unlike in Si-MOSFETs, in graphene the valley dynamics is governed by two characteristic times, the intervalley scattering time τ_i and intravalley dephasing time[10] τ_*. In our experiments, the intervalley scattering rate $\hbar/\tau_i$ is of the order of 3 K, while the intravalley dephasing rate is above 20 K (see Table I). Thus the intermediate regime, $\hbar/\tau_i < k_BT < \hbar/\tau_*$, becomes possible. In this case, the channels with two electrons from different valleys give no contribution. (This situation is similar to the one which occurs for universal conductance fluctuations in graphene.[23]) As there are two spin states per electron and two states for two electrons in the same valley, there are eight remaining channels, one of which is both spin and valley singlet, so that $c=7$. Thus we arrive at the following expression for A in Eq. (1)

$$A(F_0^\sigma) = 1 + 7[1 - \ln(1+F_0^\sigma)/F_0^\sigma]. \tag{5}$$

We have confirmed this analysis by standard diagrammatic calculations, where we used a common assumption that all channels except for the singlet are described by the same Fermi-liquid parameter.

Using Eq. (5) and the experimental values of A, Fig. 4, we find the values of F_0^σ to be between -0.07 and -0.14. It is interesting to note that the value of F_0^σ found in GaAs and Si systems at $r_s \sim 1$ is between -0.15 and -0.2.[4,7,8] To explain this relatively low value of $F_0^\sigma \approx -0.1$ found in our experiments, we note that in graphene this constant is suppressed due to the chirality of charge carriers, which prevents large-angle electron-electron scattering. In a nonchiral system, the constant F_0^σ can be found by averaging the electron-electron scattering amplitude over all possible scattering angles (see, e.g., Ref. 2): $F_0^\sigma = -\nu\langle U(|\mathbf{p}-\mathbf{p}'|)\rangle$. Here $U(q)$ is the Fourier component of the interaction potential and ν is the density of electron states per spin/valley. In a chiral system, the scattering amplitude for each electron is suppressed by the factor $\cos(\theta/2)$, where θ is the scattering angle (see, e.g., Ref. 13), so that $F_0^\sigma = -\nu\langle U(|\mathbf{p}-\mathbf{p}'|)\cos^2(\theta/2)\rangle$.

For a simple estimate away from the Dirac point, we use the Thomas-Fermi approximation for the interaction potential, $U(q)=2\pi e_*^2/(q+\kappa)$, with the effective charge, $e_*^2 = 2e^2/(\epsilon+1)$ that includes suppression of the Coulomb interaction by the SiO_2 substrate, $\epsilon=3.9$. The screening parameter $\kappa = 4\times 2\pi\nu e_*^2$ includes contributions from four degenerate single-electron states (in graphene the density of electron states is $\nu = E_F/2\pi v_F^2$). This gives

$$F_0^\sigma = -\alpha\int_0^\pi \frac{d\theta}{\pi}\frac{\cos^2\frac{\theta}{2}}{2\sin\frac{\theta}{2}+2\alpha}, \tag{6}$$

where $\alpha = e_*^2/\hbar v_F \approx 0.88$ is the dimensionless interaction constant (it is related to the parameter r_s used in Refs. 3–8 as $r_s=\sqrt{2}\alpha$). Evaluating this integral, we find $F_0^\sigma = -0.10$, which is in agreement with our measurements. Note, that a similar calculation for a nonchiral electron liquid with two valleys gives a larger value $F_0^\sigma \approx -0.19$ for the same value of α. Approximation (6) which neglects effects of strong interaction, such as the Fermi velocity and Z factor renormalizations,[24] is expected to be valid for $\alpha \leq 1$, which is the case for graphene. Our result is in agreement with the value of F_0^a in Ref. 24 for the studied range of charge densities. (To compare F_0^σ with F_0^a in Ref. 24, one has to take into account that these quantities are related as $F_0^a = 2F_0^\sigma$.)

In summary, we show that electron-electron interaction plays an important role in the low-temperature conductivity of carriers in graphene. Unexpectedly for the EEI correction, its magnitude is affected by the intravalley decoherence rate due to elastic scattering. We find the value of the interaction parameter F_0^σ in graphene, which is lower than in other 2D systems studied earlier.

ACKNOWLEDGMENTS

We are grateful to V. I. Fal'ko, A. D. Mirlin, E. McCann, I. V. Lerner, M. Polini, and D. W. Horsell for useful discussions, and to R. V. Gorbachev and F. V. Tikhonenko for support in fabricating samples. We would like to thank the EPSRC (Grant No. EP/G036101/1) for funding.

[1] G. Bergmann, Phys. Rep. **107**, 1 (1984).

[2] B. L. Altshuler and A. G. Aronov, in *Electron-Electron Interactions in Disordered Systems*, edited by A. L. Efros and M. Pollak (North-Holland, Amsterdam, 1985).

[3] G. Zala, B. N. Narozhny, and I. L. Aleiner, Phys. Rev. B **64**, 214204 (2001).

[4] Y. Y. Proskuryakov, A. K. Savchenko, S. S. Safonov, M. Pepper, M. Y. Simmons, and D. A. Ritchie, Phys. Rev. Lett. **89**, 076406 (2002); A. K. Savchenko, E. A. Galaktionov, S. S. Safonov, Y. Y. Proskuryakov, L. Li, M. Pepper, M. Y. Simmons, D. A. Ritchie, E. H. Linfield, and Z. D. Kvon, Phys. Status Solidi B **242**, 1204 (2005).

[5] A. A. Shashkin, S. V. Kravchenko, V. T. Dolgopolov, and T. M. Klapwijk, Phys. Rev. B **66**, 073303 (2002).

[6] V. M. Pudalov, M. E. Gershenson, H. Kojima, G. Brunthaler, A. Prinz, and G. Bauer, Phys. Rev. Lett. **91**, 126403 (2003).

[7] S. A. Vitkalov, K. James, B. N. Narozhny, M. P. Sarachik, and T. M. Klapwijk, Phys. Rev. B **67**, 113310 (2003).
[8] N. N. Klimov, D. A. Knyazev, O. E. Omel'yanovskii, V. M. Pudalov, H. Kojima, and M. E. Gershenson, Phys. Rev. B **78**, 195308 (2008).
[9] H. Suzuura and T. Ando, Phys. Rev. Lett. **89**, 266603 (2002).
[10] E. McCann, K. Kechedzhi, Vladimir, I. Fal'ko, H. Suzuura, T. Ando, and B. L. Altshuler, Phys. Rev. Lett. **97**, 146805 (2006).
[11] F. V. Tikhonenko, D. W. Horsell, R. V. Gorbachev, and A. K. Savchenko, Phys. Rev. Lett. **100**, 056802 (2008).
[12] F. V. Tikhonenko, A. A. Kozikov, A. K. Savchenko, and R. V. Gorbachev, Phys. Rev. Lett. **103**, 226801 (2009).
[13] V. V. Cheianov and V. I. Fal'ko, Phys. Rev. Lett. **97**, 226801 (2006).
[14] T. Ando, T. Nakanishi, and R. Saito, J. Phys. Soc. Jpn. **67**, 2857 (1998).
[15] K. S. Novoselov, A. K. Geim, S. V. Morozov, D. Jiang, M. I. Katsnelson, I. V. Grigorieva, S. V. Dubonos, and A. A. Firsov, Nature (London) **438**, 197 (2005).
[16] S. V. Morozov, K. S. Novoselov, M. I. Katsnelson, F. Schedin, D. C. Elias, J. A. Jaszczak, and A. K. Geim, Phys. Rev. Lett. **100**, 016602 (2008).
[17] J. H. Chen, C. Jang, S. Xiao, M. Ishigami, and M. S. Fuhrer, Nat. Nanotechnol. **3**, 206 (2008).
[18] T. Stauber, N. M. R. Peres, and F. Guinea, Phys. Rev. B **76**, 205423 (2007); E. H. Hwang and S. Das Sarma, *ibid.* **77**, 115449 (2008).
[19] C. R. Dean, A. F. Young, I. Meric, C. Lee, L. Wang, S. Sorgenfrei, K. Watanabe, T. Taniguchi, P. Kim, K. L. Shepard, and J. Hone, arXiv:1005.5917 (unpublished).
[20] In Ref. 17 the authors fitted high-T resistivity data with two phonon contributions: linear in T, Eq. (3), and nonlinear, which depends on the carrier density. Following their analysis we take into account the nonlinear term and fit our results of $\rho(T)$ at $T > 20$ K. The fitting procedure gives $D_a = 18$ eV for sample S1 [in region I in addition to the phonon contribution, the high-T weak antilocalization correction (Ref. 12) should be taken into account].
[21] H.-P. Wittmann and A. Schmid, J. Low Temp. Phys. **69**, 131 (1987); Y. Y. Proskuryakov, A. K. Savchenko, S. S. Safonov, M. Pepper, M. Y. Simmons, and D. A. Ritchie, Phys. Rev. Lett. **86**, 4895 (2001); K. E. J. Goh, M. Y. Simmons, and A. R. Hamilton, Phys. Rev. B **77**, 235410 (2008).
[22] Y. Zhang, Z. Jiang, J. P. Small, M. S. Purewal, Y.-W. Tan, M. Fazlollahi, J. D. Chudow, J. A. Jaszczak, H. L. Stormer, and P. Kim, Phys. Rev. Lett. **96**, 136806 (2006).
[23] M. Yu. Kharitonov and K. B. Efetov, Phys. Rev. B **78**, 033404 (2008); K. Kechedzhi, O. Kashuba, and V. I. Fal'ko, *ibid.* **77**, 193403 (2008).
[24] M. Polini, R. Asgari, Y. Barlas, T. Pereg-Barnea, and A. H. MacDonald, Solid State Commun. **143**, 58 (2007).